# Mechanistic-Empirical Pavement Design; A Brief Overview

A. T. Papagiannakis
*Department of Civil and Environmental Engineering, University of Texas at San Antonio, TX, USA*
*E-mail*: at.papagiannakis@utsa.edu

**ABSTRACT:** This paper provides an overview of the state of the art of mechanistic-empirical pavement design, as established by NCHRP Study 1-37A in the United States. It describes the method used to characterize traffic loading and materials, as well as the methods used to analyse flexible and rigid pavement response and calculate damage. This methodology is referred as the Mechanistic-Empirical Pavemnt Design Guise (MEPDG) and was recently implemented into the commercially available software referred to as the *AASHTOWare* Pavement Mechanistic Empirical Design.

## 1. INTRODUCTION

The information presented in this paper is based on the work conducted under NCHRP Study 1-37A (NCHRP 2004), which was recently adopted by the American Association of State Highway and Transportation Officials (AASHTO) as the design software *AASHTOWare* Pavement Mechanistic-Empirical Design (AASHTO 2012). It supersedes the earlier empirical pavement design approach (AASHTO 1993). The new method, hence referred to as the ME PDG, is based on disaggregate axle load information (i.e., load spectra), structural response to load calculations, accumulation of damage due to traffic and environment and finally translation of these predictions to performance measures (e.g., cracking, rutting and so on) versus age. The temporal distribution in traffic loads is considered in monthly increments, while environmental data is used to project design period temperature and moisture effects on material properties. The following sections provide a brief overview of the main features of this design approach. More detail can be found in manual of practice published by AASHTO (2008) and instructional material in a recent textbook by Papagiannakis and Masad (2008).

## 2. INSTRUCTIONS

Traffic loads are characterized in terms of load spectra, that is the actual number of applications by axle configuration and load level by month. In practice, this information is synthesized by combining traffic counts, vehicle classification information and axle load data obtained by automated vehicle counters, classifiers (AVC) and weigh-in-motion (WIM) systems, respectively. The type of traffic data used to synthesize the load spectra defines the traffic input Level (Table 1).

Table 1 Traffic Input Levels to the ME PDG

| Data Element/Input Variables | Traffic Input Level | | |
|---|---|---|---|
| | 1 | 2 | 3 |
| Axle Load Data (WIM) – Site/Segment Specific | x | | |
| Axle Load Data (WIM) – Regional Measured | | x | |
| Axle Load Data (WIM) – Regional or National Default | | | x |
| Vehicle Classification Data (AVC) – Site/Segment Specific | | x | |
| Vehicle Classification Data (AVC) – Regional Measured | | x | |
| Vehicle Classification Data (AVC) – Regional or National Default | | | x |
| Traffic counts/Percent trucks | | | x |

Examples of load spectra are shown in Figures 1 and 2.

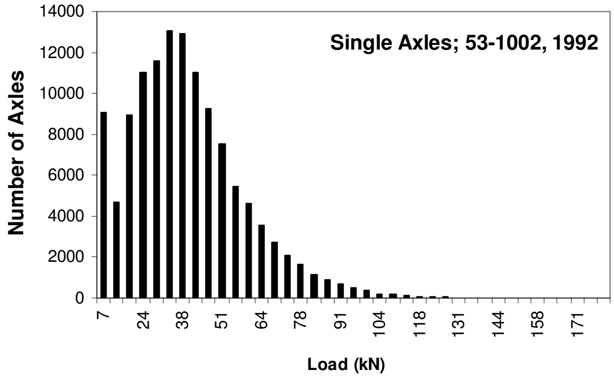


Figure 1 Example of an annual load spectrum for single axle

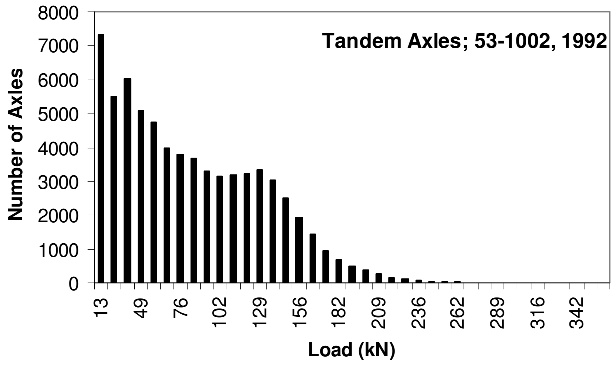


Figure 2 Example of an annual load spectrum for tandem axles

Traffic is input in the form of Average Annual Truck Traffic (AADTT) volumes involving FHWA (2001) vehicle classes 4 to 13 (buses to multi-unit trailer trucks, resp.). They are monthly adjusted though Monthly Adjustment Factors (MAFs) defined as the ratio of the volume in a particular month divided by the AADTT for this month by vehicle class. The distribution of axle loads by axle configuration (i.e., single, tandem, triple and quad) is compiled from WIM data output.

For design sites where AVC and WIM data is not available (i.e., traffic input Levels 2 and 3), the necessary data can be estimated by associating the design site with other similar traffic data collection sites where such data is available. This is done objectively using clustering techniques (Papagiannakis et al., 2006). This is possible where some short-term site-specific data can be obtained. If this is not possible, design will have to rely on Level 3 traffic input, which utilizes subjective means of obtaining vehicle classification (e.g., urban arterial, rural interstate and so on), temporal traffic distribution (i.e., all MAF values equal to 1.0) and axle load distribution (national average values). This type of information constitutes Level 3 traffic input defaults and it is incorporated as default values in the *AASHTOWare* software. As pointed out later, lack of site-specific WIM and AVC data of sufficient length coverage significantly affects pavement performance predictions.

## 3. CLIMATIC MODEL

The ME PDG incorporates a comprehensive climatic model that estimates the temperature and moisture distribution within the pavement layers utilizing as input ambient air temperature, solar radiation/wind and precipitation/evaporation data. The model adopted for this purpose is the Enhanced Integrated Climatic Model (EICM) (Lytton et al., 1993). This combines the Climatic-Materials-Structural (CMS) model developed by Dempsey et al., (1985) and the Infiltration Design (ID) model developed by Liu et al., (1986). These models use finite-difference algorithms to solve the one-dimensional heat and moisture diffusion in pavements, respectively. Large amounts of climatic data were incorporated into the MEPDG software from over 800 weather stations across the United States covering a period longer than 10 years. This model allows estimating the temperature and moisture distributions in the pavement layers for the typical day in each month at location defined by its latitude and longitude. As pointed out next, this data is used to estimate seasonal layer moduli, the resulting pavement responses from traffic load applications as well as the thermal stresses imposed on asphalt and Portland concrete layers.

## 4. FLEXIBLE PAVEMENT ANALYSIS

### 4.1 The Flexible Structure Model

Flexible pavement structural response calculations are carried out using the layer elastic analysis software package JULEA (Uzan 2001). Estimates of pavement response are obtained for each axle load interval and each season (i.e., five temperature quintiles in each month). Strains associated with the damage models described next are stored and used for estimating:

- Asphalt concrete fatigue cracking (bottom-up and top-down)
- Asphalt concrete and granular layer plastic deformation
- Transverse thermal cracking and
- Rutting and,
- Roughness

Each of these damage models is described next. The material characterization required for these models is classified into three hierarchical levels. Level 1 requires detailed material testing. For the asphalt concrete, for example, the $E^*$ master curve and the creep or repetitive cycling properties are required, while for the base layers, resilient and plastic deformation properties are required. Level 2 utilizes empirical relationships between index properties (e.g., volumetric asphalt concrete properties) and fundamental mechanical properties (e.g., $E^*$ master curve). Level 3 analysis, relies on national average default material properties built into the ME PDG software. This allows conducting the ME PDG analysis with limited testing. As pointed out later, however, the quality of material input significantly affects the quality of the pavement performance predictions obtained.

### 4.2 Flexible Damage Model

#### 4.2.1 Fatigue model

The fatigue model used has the format used by Asphalt Institute's flexible pavement design approach (Asphalt Institute 1981):

$$N_f = 0.007566\, k_1'\, C \left(\frac{1}{\varepsilon_t}\right)^{3.9492} \left(\frac{1}{E}\right)^{1.281} \qquad (1)$$

where $N_f$ is the number of cycles to failure, $\varepsilon_t$ is the tensile strain in the asphalt concrete layer and $E$ is the layer stiffness (lbs/in$^2$). The coefficients $C$ and $k_1'$ are calibration constants.

Fatigue damage $FD$ (percent) is accumulated separately for bottom-up and top-down cracking according to Miner's hypothesis expressed as:

$$FD = \sum \frac{n_{i,j,k,l,m}}{N_{i,j,k,l,m}} 100 \qquad (2)$$

where,
$n_{i,j,k,\ldots}$ = number of actual load applications at condition *i, j, k, l, m, n,*
$N_{i,j,k,\ldots}$ = number of axle load applications to cracking failure under conditions *i, j, k, l, m,* where,
$i$ = month, which accounts for monthly changes in the moduli of base and subgrade due to moisture variations and asphalt concrete due to temperature variations,
$j$ = time of the day, which accounts for hourly changes in the modulus of the asphalt concrete,
$k$ = axle type, (i.e., single, tandem, triple and quad),
$l$ = load level for each axle type,
$m$ = traffic path, assuming a normally distributed lateral wheel wander. An example of the annual $n_{i,j,k}$ applications was shown in Figures 1 and 2 respectively. The resulting pavement wheel path length cracked in fatigue (feet/mile) is calculated using:

$$FC = \frac{10560}{1 + e^{(7.0 - 3.5 \log FD)}} \qquad (3)$$

#### 4.2.2 Plastic deformation (rutting) models

Rutting is estimated by summing the plastic deformation in the asphalt concrete and granular layers (base and subgrade):

$$PD = \sum_{i=1}^{n} \varepsilon_p^i\, h^i \qquad (4)$$

where, $\varepsilon_p^i$ is the plastic strain in layer $i$, $h^i$ is the thickness of the layer $i$ and $n$ is the number of layers.

For the asphalt concrete layer, the plastic strain $\varepsilon_p$ is estimated as a function of the elastic (recoverable) strain $\varepsilon_v$ using:

$$\frac{\varepsilon_p}{\varepsilon_v} = k_1 10^{-3.35412}\, T^{1.5606} N^{0.479244} \qquad (5)$$

where, $T$ is the asphalt concrete layer temperature (ºF), $N$ is the cumulative number of loading cycles experienced and $k_1$ is a calibration factor accounting for the increased level of confinement with depth.

For granular layers, plastic strain is calculated using a model developed by Tseng and Lytton (1989):

$$\frac{\varepsilon_p}{\varepsilon_v} = \beta_G \left(\frac{\varepsilon_0}{\varepsilon_r}\right) e^{-\left(\frac{\rho}{N}\right)^{\beta}} \qquad (6)$$

where, $\beta$, $\rho$ and $\varepsilon_0$ are material properties obtained from laboratory testing involving repetitive loading at resilient strain level $\varepsilon_r$ and $N$ is the number of load cycles. The calibration constant $\beta_G$ has the value of 1.673 for base layers and 1.35 for subgrades. The values of $\beta$ and $\rho$ are given by:

$$\log \beta = -0.6119 - 0.017638\, W_c \qquad (7)$$

$$\rho = 10^9 \left( \frac{-4.89285}{1-(10^9)^{\beta}} \right)^{\frac{1}{\beta}} \tag{8}$$

where $W_c$ is the water content (%).

### 4.2.3 Transverse thermal cracking model

The thermal cracking model adopted by the ME PDG is based on work carried out under Strategic Highway Research Program (SHRP) contract A-005 (Von Quintus 1994) and the work carried out by Witczak et al. (2000). Its basic mechanism relates the thermal stresses computed from the creep compliance of the asphalt concrete to its tensile strength. The properties are determined by the Indirect Tension (IDT) test conducted according to AASHTO Standard T322-03. The IDT test is used to measure the creep compliance of the asphalt concrete in tension at various temperatures and construct its master curve. Transforming this function into the frequency domain allows estimating the stress relaxation modulus of the asphalt concrete in the frequency domain. This allows computing stresses as a function of changing temperature and/or loading time using Boltzman's superposition principle. Cracks are formed when thermal stresses exceed asphalt concrete tensile strength. Crack propagation is modelled using Paris' Law (Paris and Erdogan, 1963):

$$\Delta C = A\ \Delta K^n \tag{9}$$

where, $\Delta C$ is the increase in crack length, $\Delta K$ is the change in the stress intensity function and $n$ and $A$ are fracture parameters. The stress intensity factor is computed using:

$$K = \sigma \left( 0.45 + 1.99\ C_0^{\ 0.56} \right) \tag{10}$$

where, $C_0$ is the original crack length and $\sigma$ is the stress in the asphalt concrete layer at the depth of the crack tip. The parameter $n$ is obtained by fitting an exponential relationship to the creep compliance master curve. It relates the cracking parameter $n$ to the slope $m$ of the linear part of master curve through:

$$n = 0.8\left(1 + \frac{1}{m}\right) \tag{11}$$

The parameter $A$ was established through calibration using in-situ transverse cracking data:

$$\log A = 4.389 - 2.52\ \log\left(10000\ S_t\ n\right) \tag{12}$$

where $S_t$ is the tensile strength (lbs/in$^2$) of the asphalt concrete mix measured as described earlier. Finally, the extent of transverse thermal cracking in asphalt concretes $TC$ (in linear feet/mile) is computed from the probability that the length of thermal cracks $C$ exceeds the thickness of the asphalt concrete layer $D$, expressed as:

$$TC = 400\, N\left(\frac{\log C/D}{0.769}\right) \tag{13}$$

### 4.2.4 Roughness Model

The roughness model is largely based on the estimates of cracking and rutting obtained with the models described above:

$$IRI = IRI_0 + 0.0150\, SF + 0.4\, FC_T + 0.0.008\, TC + 40.0\, RD \tag{14}$$

where, $IRI_0$ is the initial (as constructed) pavement roughness, $FC_T$ is the percent of the total pavement surface area cracked, $TC$ is the total length of transverse cracking (ft/mile) and $RD$ is the average rut depth (inches), and $SF$ is a site factor computed as:

$$SF = Age\left[0.02003(PI+1) + .007947(Precip+1) + 0.000636(FI+1)\right] \tag{15}$$

where, $Age$ is the age of the pavement in years, $PI$ is the plasticity index of the subgrade, $Precip$ is the average annual precipitation (inches) and $FI$ is the freezing index (ºF-days). Clearly, the flexible pavement roughness model is largely empirical.

## 5. RIGID PAVEMENT ANALYSIS

### 5.1 The Rigid Structural Model

The ME PDG uses the 3-D finite element program ISLAB 2000 (Khazanovich et al., 2000) to estimate the structural response of Portland concrete pavements. Temperature profiles are computed at 11 equally spaced depth increments into slabs at hourly intervals, based on climatic data from the weather station nearest to the pavement design location. The effect of relative humidity is translated into an equivalent temperature gradient. Stresses are computed for a limited combination of axle locations and slab conditions, including:

- Slab curling due to temperature/moisture gradients,
- Loss of subgrade support due to curling,
- Slab-to-slab interaction.

Each of these damage functions is described next. This output is fed into a neural-network algorithm for estimating the critical structural response parameters to be input into the pavement damage functions. The material properties for these models are similarly classified into three hierarchical levels as for flexible pavements.

### 5.2 The Rigid Damage Models

The ME PDG considers the following damage mechanisms:

- Fatigue transverse cracking, both bottom-up and top-down, for jointed concrete pavements (JCPs) only,
- Joint faulting for JCPs only,
- Punch-outs for continuously reinforced concrete pavements (CRCPs) only and,
- Roughness for both JCP and CRCP pavements.

Each is discussed briefly next.

### 5.2.1 Fatigue transverse cracking model

Fatigue cracking (bottom-up and top-down) for rigid pavements is accumulated using Miner's Hypothesis (Equ. 2). The parentage of bottom-up and top-down cracking denoted as $CRK_p$, $CRK_q$, respectively, is given by:

$$CRK_{p,q} = \frac{1}{1 + FD_{p,q}^{\ -1.98}} \tag{16}$$

while, the total percentage of slab cracking $TCRACK$ is given by:

$$TCRACK = \left(CRK_p + CRK_q - CRK_p CRK_q\right)100\% \tag{17}$$

and the number of cycles to failure is given by:

$$\log\left(N_{i,j,k,l,m,n}\right) = 2.0\left(\frac{MR_i}{\sigma_{i,j,k,l,m,n}}\right)^{1.22} - 1 \tag{18}$$

where, $MR_i$ is the modulus of rupture of Portland concrete at age $i$ (lb/in$^2$).

### 5.2.2 Joint faulting model

Faulting in JCPs is computed using an incremental approach, whereby the faulting increments by month $i$, $\Delta Fault_i$, are summed to compute the total faulting after $m$ months, $Fault_m$, (inches):

$$Fault_m = \sum_{i=1}^{m} \Delta Fault_i \tag{19}$$

For each month, the faulting increment, $\Delta Fault_i$ is assumed proportional to the energy dissipated in deforming the slab support, expressed as:

$$\Delta Fault_i = C_{34} \left(FAULTMAX_{i-1} - Fault_{i-1}\right)^2 DE_i \tag{20}$$

where, $Fault_{i-1}$ is the accumulated mean faulting up to the previous month $i$-1, $FAULTMAX_{i-1}$ is the maximum mean faulting for the previous month, $i$-1, $DE_i$ is the differential energy of subgrade deformation and $C_{34}$ is a function of the percent time the base layer is below freezing. Assuming a liquid foundation with a modulus of subgrade reaction $k$, allows computing the energy input into the subgrade as:

$$DE = \frac{1}{2} k \left(w_l^{\,2} - w_{ul}^{\,2}\right) \tag{21}$$

where, $w_l$ and $w_{ul}$ are the surface vertical deflections of the loaded (i.e., leave) slab and unloaded (i.e., approach) slab, respectively. $DE$ is a function of the Load Transfer Efficiency ($LTE$) of a joint:

$$DE = \frac{1}{2} k \left(w_l + w_{ul}\right)\left(w_l - w_{ul}\right) = \frac{1}{2} k \left(w_l + w_{ul}\right)^2 \frac{1 - \frac{LTE}{100}}{1 + \frac{LTE}{100}} \tag{22}$$

Depending on the joint configuration, (i.e., plain or dowel-reinforced), $LTE$ is calculated as:

$$LTE_{joint} = 100\left(1 - \left\{1 - \frac{LTE_{dowel}}{100}\right\}\left\{1 - \frac{LTE_{agg}}{100}\right\}\left\{1 - \frac{LTE_{base}}{100}\right\}\right) \tag{23}$$

where, $LTE_{agg}$, $LTE_{dowel}$ and $LTE_{base}$ is the load transfer efficiency from aggregate interlock, dowel action and base support, respectively. They are computed from the size of the joint opening, the geometry/condition of slab/dowel and the base type, respectively.

For the first month, the pavement is opened to traffic, faulting is computed as:

$$FAULTMAX_0 = C_{12}\, \delta_{curling} \left[\log\left(1 + 250\, 5.0^{EROD}\right) \log\left(\frac{P_{200}\, WetDays}{P_s}\right)\right]^{0.4} \tag{24}$$

where $C_{12}$ is a function of the percent time the base layer is below freezing, $\delta_{curling}$ is the maximum mean monthly slab corner upward deflection, (inches), due to temperature and moisture gradients, $EROD$ is an index of the erosion potential of the slab support, (i.e., ranges from 1 for stabilized bases with geotextiles and drainage to 5 for slab on grade), $P_s$ is the overburden stress on the subgrade (lb/in$^2$), $P_{200}$ is the percent of subgrade sizes finer than sieve No. 200 (0.075 mm) and, $WetDays$ is the average annual number of wet days, (i.e., daily rainfall higher than 0.1 in). In subsequent months, faulting is calculated using:

$$FAULTMAX_i = FAULTMAX_0 + 1.2 \sum_{j=1}^{m} DE_j \, \log\left(1 + 250\, 5.0^{EROD}\right)^{0.4} \tag{25}$$

### 5.2.3 Punch-out model

Punchouts in continuously reinforced Portland concrete pavements are the result of the formation of longitudinal top-down fatigue cracks spanning two adjacent transverse cracks. They typically occur near the edge of a driving lane, when the upper surface of the pavement is concave and when the load transfer between slab and shoulder is poor. Estimating the occurrence of punchouts involves a number of steps:

- Estimate mean transverse crack spacing and opening
- Estimate LTE across these cracks

Crack spacing is important because it affects crack width, which in turn affects $LTE$ across the crack. The mean transverse crack spacing (inches) is calculated using:

$$\bar{L} = \frac{f_t - C\sigma_0\left(1 - \frac{2\zeta}{h}\right)}{\frac{f}{2} + \frac{u_m\, p}{c_1 d}} \tag{26}$$

where, $f_t$ is the Portland concrete tensile strength (lb/in$^2$), $f$ is the coefficient of friction between slab and supporting layer, $u_m$ is the maximum bond stress between steel bars and concrete (lb/in$^2$), $p$ is the ratio of steel reinforcement area divided by slab cross sectional area, (percent), $d$ is the reinforcing steel bar diameter (inches), $h$ is the slab thickness (inches), $\zeta$ is the depth to steel reinforcement location (inches) and, $C$ is Bradbury's curling/warping stress coefficient computed for the typical lane width of 144 inches. The bond slip coefficient $c_1$ is given by:

$$c_1 = 0.577 - 9.499\, 10^{-9} \frac{\ln \varepsilon_{tot-\varsigma}}{\left(\varepsilon_{tot-\varsigma}\right)^2} + 0.00502\, \bar{L} \ln\left(\bar{L}\right) \tag{27}$$

where, $\varepsilon_{tot-\varsigma}$ is the total strain (in/in) at the depth $\zeta$ of the steel reinforcement, caused by temperature gradient and shrinkage for the current month, $\sigma_0$ is Westergard's nominal stress factor:

$$\sigma_0 = \frac{E\ \Delta\varepsilon_{tot}}{2(1-\mu)} \tag{28}$$

with, $E$ and $\mu$ the young's modulus and Poison's ratio, $\Delta\varepsilon_{tot}$ the equivalent unrestrained curling/warping strain difference between top and bottom of slab (in/in) as a result of the temperature/moisture gradient for the current month.

The corresponding average crack width, $c\overline{w}$ (0.001 inches) at the level of steel reinforcement is:

$$c\overline{w} = \bar{L}\left(\varepsilon_{shr} + \alpha_t\, \Delta T_\varsigma - \frac{c_2\, f_\sigma}{E}\right)1000 \tag{29}$$

where, $\varepsilon_{shr}$ is the unrestrained concrete drying shrinkage at the depth of the reinforcement (in/in $10^{-6}$),$\alpha_t$ is the Portland concrete coefficient of thermal expansion (/°F), $\Delta T_\zeta$ is the difference in Portland concrete temperature between the monthly mean temperature and its "set" temperature at the depth of the steel $\zeta$ (°F), $f_\sigma$ is the maximum longitudinal tensile stress in the Portland concrete at the steel level (lb/in$^2$), and, $c_2$ is another bond slip coefficient. The average crack width, $\overline{cw}$, allows computing the dimensionless shear transfer capacity of the crack due to aggregate interlock, *s* as:

$$s = 0.05\, h\ \exp\left(-0.032\, \overline{cw}\right) \tag{30}$$

which in turn allows computing the combined crack stiffness $J_c$ from aggregate interlock:

$$\log(J_c) = -2.2\exp\left\{-2.718^{-\frac{J_s+11.26}{7.56}}\right\} - 28.85\exp\left\{-2.718^{-\frac{s-0.35}{0.38}}\right\} + 49.8\exp\left\{-2.718^{-\frac{J_s+11.26}{7.56}}\right\}\exp\left\{-2.718^{-\frac{s-0.35}{0.38}}\right\} \tag{31}$$

Finally, the $LTE_c$ across CRCP cracks is computed as:

$$LTE_c = \frac{100}{1+10^{\left(\frac{0.214-0.183\frac{a}{l}-\log(J_c)-R}{1.18}\right)}} \tag{32}$$

Finally, the number of punchouts, *PO*, (number per mile), is computed using:

$$PO = \frac{106.3}{1+4.0\ FD^{-0.4}} \tag{33}$$

where, *FD* is the fatigue damage accumulated (Equ. 2).

### 5.2.4 Roughness model

For JCPs, roughness (IRI in/mi) is estimated as a function of the distress predictions, namely fatigue cracking, faulting and spalling, as well as the initial, (i.e., post-construction) roughness. Spalling is predicted on the basis of the following empirical expression:

$$SPALL = \left[\frac{AGE}{AGE+0.01}\right]\left[\frac{100}{1+1.005^{(-12\,AGE+SCF)}}\right] \tag{34}$$

*SPALL* is the percent of joints with medium/high severity spalling, *AGE* is the pavement age (years) and *SCF* is a scaling factor given by:

$$SCF = -1400 + 350\ AIR\%\ (0.5+PREFORM) + 1.36\ f_c' - 0.2\ FTCYC\ AGE + 43\ h - 536\ WC\_RATIO \tag{35}$$

Roughness, is given by:

$$IRI = IRI_i + 0.0823\ CRK + 0.4417\ SPALL + 1.4929\ TFAULT + 25.24\ SF \tag{36}$$

where *SF* is site factor given my:

$$SF = AGE\ (1+0.5556\ FI)\frac{1+P_{200}}{10^6} \tag{37}$$

For CRCPs, roughness (*IRI* in in/mi), is expressed as a function of the post-construction *IRI*, pavement age as reflected by the site factor *SF* (Equ. 37) and the number of punchouts (*PO*) estimated earlier (Equ. 33):

$$IRI_m = IRI_i + 3.15\ PO + 28.35\ SF \tag{38}$$

Clearly, the rigid pavement roughness models are also largely empirical, as was the case for the flexile pavement models.

## 6. MODEL CALIBRATION

The pavement damage functions described above were calibrated during the development of the ME PDG using field performance observations from three large scale pavement experiments, namely the Minnesota Road Research (MnROAD) Project, the WesTrack Project and the Long Term Pavement Performance (LTPP) Program. The MnROAD Project is a heavily instrumented 6-mile long section of I-94 located 64 km northwest of Minneapolis / St.Paul. Instrumentation ranged from pavement strain/stress gauges to subgrade temperature/moisture gauges numbering to more than 4500 in total. Both flexible and rigid pavements were tested under in-service traffic monitored by WIM systems.

The WesTrack is 2.9 km long oval test track located 100 km southeast of Reno on the grounds of the Nevada Automotive Research Center. It was designed to test the performance of a number of alternative asphalt concrete mix designs and evaluate the effect of variations in structural design and material properties (e.g., asphalt content, air void content, and aggregate gradation). Traffic was applied by means of 4 driverless triple-trailer trucks that applied a total of 10 million ESALs over a period of 2 years.

The LTPP is a large scale experiment initiated in 1986 as part of the Strategic Highway Research Program (SHRP). It involves a large number of 150-m long test sections across the US and Canada. Experiments involved existing pavement and purpose-built pavement sections designated as General Pavement Sections (GPS) and Special Pavement Sections (SPS), respectively. The total of number of sections was approximately 652 and 1262, respectively. These sections were exposed to in-service traffic monitored by WIM systems. Pavement data has been collected at these sections for over 20 years through four regional contracting agencies under the oversight of the FHWA. The data is assembled into a massive database, which is being periodically released to the public under the DataPave database label. This database includes data on a multitude of inventory, material, traffic, environmental and pavement evaluation variables.

Currently, individual State Highway Departments are in the process of further calibrating these damage models to better match the predictions of the ME PDG to regionally observed data. The ME PDG software allows this type of "fine-tuning" by allowing adjustments of the majority of the coefficients in the damage models described earlier by applying dimensionless factors which in their default format are equal to 1.00.

## 7. MODEL SENSITIVITY

A multitude of studies have pointed out the significant sensitivity of the ME PDG to traffic input. For example, Papagiannakis et al. (2006) showed significant pavement life prediction errors, for traffic input scenarios based on moving away from site-specific information and decreasing the length of time coverage for the data available. These errors were calculated with reference to continuous coverage site-specific WIM data. The scenarios tested are as follows:

1. Site-specific WIM data.
2. Site-specific classification and regional axle load spectra (i.e., regional set selected through clustering techniques).
3. Site-specific volume counts, regional classification and axle load frequencies (i.e., regional set selected through clustering techniques).
4. Site-specific volume counts, national average classification and load spectra (default ME PDG values).

Each of these scenarios was further subdivided by length of data coverage (e.g., 1 indicates 1 month for each of 4 seasons, 2 indicates 1 week for each of 4 seasons and so on). Figures 3 and 4 show the potential errors in ME PDG pavement life predictions for mean input and low percentile input in all traffic input parameters, respectively. Errors as high as 200% in pavement life predations are possible compared to the pavement life predictions obtained using continuous site-specific WIM data coverage. Such analyses point out the importance of site-specific high quality classification and load data in pavement design.

More recently, the sensitivity of the ME PDG was examined with respect to a broad range of material and other input properties. An example of the output of one of these studies for flexible pavement is shown in Figures 5 and 6, where the horizontal axis signifies the elasticity, (i.e., the precent change in one of the distress predictions in response to a unit precent change in one of the input).

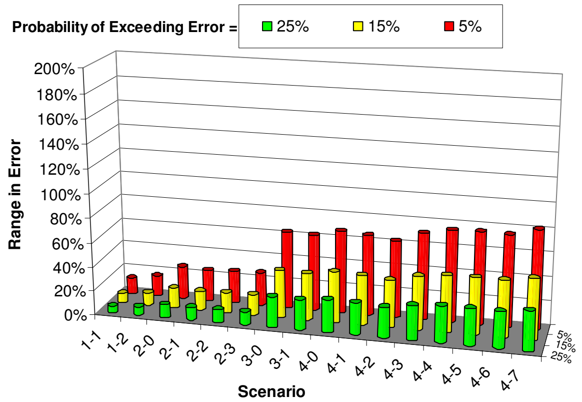


Figure 3 Potential errors in MEPDG pavement life predictions using the mean values for all traffic input (Papagiannakis et al., 2006)

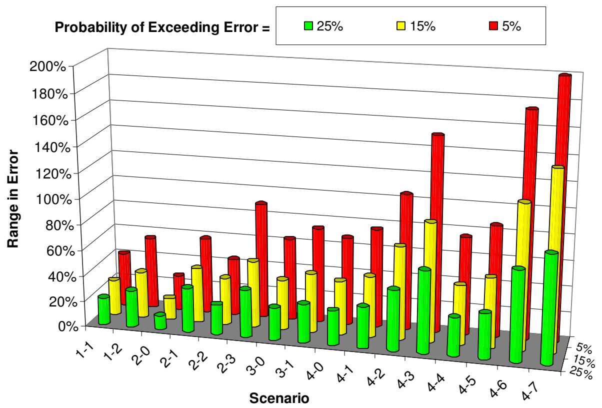


Figure 4 Potential errors in MEPDG pavement life predictions using the low percentile input for all traffic input (Papagiannakis et al., 2006)

These figures suggest higher sensitivity of the ME PDG fatigue cracking and rutting predictions to the parameters that define the asphalt concrete stiffness master curve rather than the thickness of the asphalt concrete layer and even less so to the truck traffic volume. Similar findings were obtained for the other distress predictions suggesting that the new design approach offers a fresh insight into the parameters a designer needs to consider for long lasting pavements.

## 8. EXAMPLE

An example of the main ME PDG traffic input screen is shown in Figure 7. Some the required information can be input manually, while larger data sets (e.g., load distribution input) can be imported from external files. Figures 8 and 9 show some of the ME PDG output, namely IRI and rutting predictions, respectively. Figure 8, for example, suggests that the IRI threshold value of 172 inches/mile is reached after 16 years, which is shorter than the 20 year analysis period. Material properties and layer thicknesses can be modified and the analysis rerun to satisfy that critical distress do not surpass the selected critical thresholds over the analysis period selected.

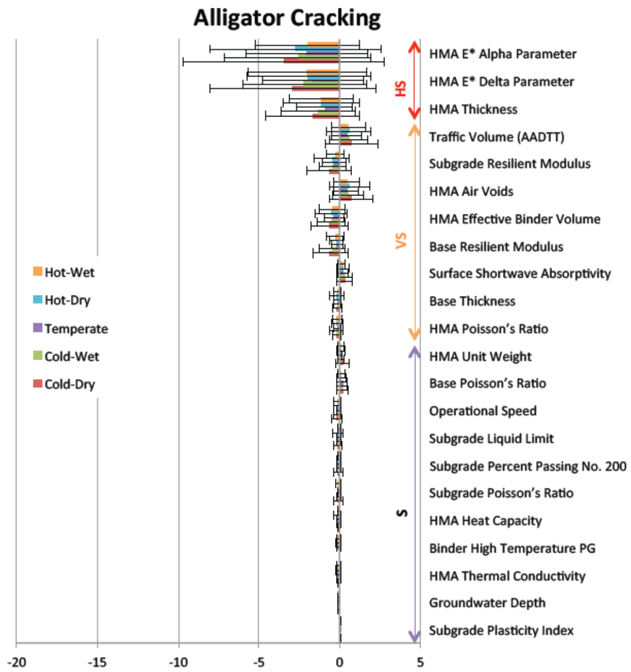


Figure 5 Sensitivity of flexible pavement alligator cracking ME PDG predictions (Schwartz et al., 2013)

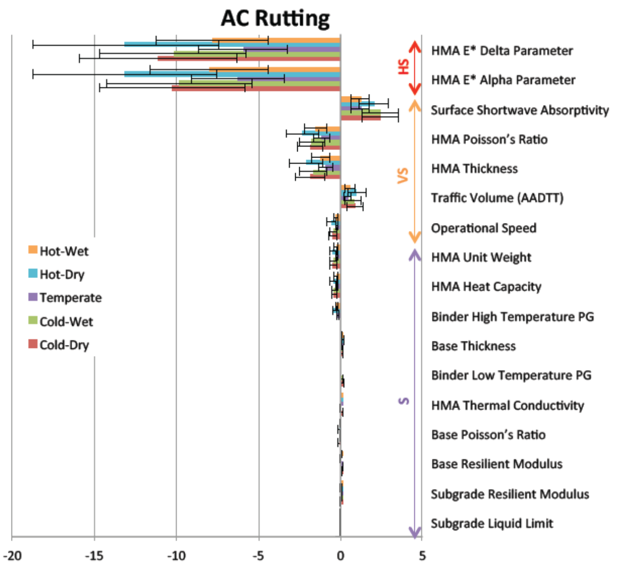


Figure 6 Sensitivity of asphalt concrete rutting ME PDG predictions (Schwartz et al., 2013)

## 9. IN SUMMARY

The brief overview presented here illustrates the significant increase in sophistication of the new ME PDG method compared to the 1993 AASHTO PDG method, which was based on two empirical performance equations, one for flexible and one for rigid pavements. The advantages of the new method are:

- Traffic loading is handled in a disaggregate fashion,
- Fundamental material properties are input
- Damage models represent the current state of the art.

Current traffic and material characterization methods, namely the wide use of WIM systems and the acceptance of Supeprpave, make the implementation of this new pavement design method feasible.

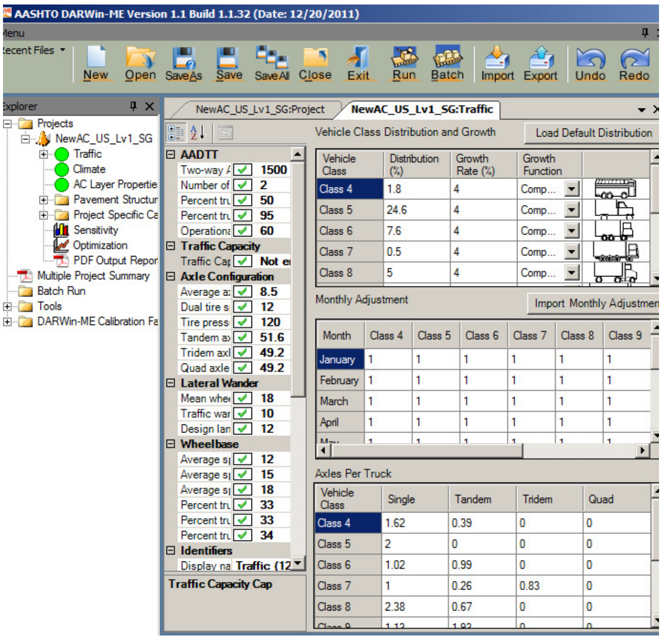


Figure 7 Example of the ME PDG traffic input interface

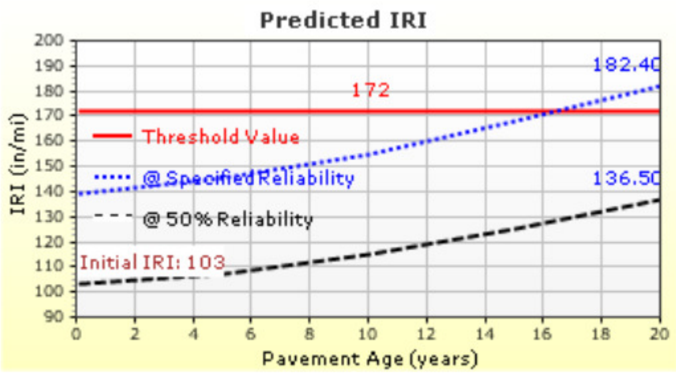


Figure 8 Example of a flexible pavement analysis; IRI predictions

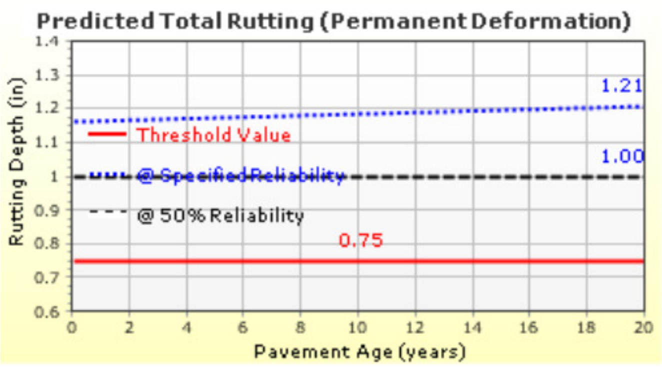


Figure 9 Example of a Flexible Pavement Analysis; Rutting Predictions.

## 10. REFERENCES


AASHTO (Dec. 2012) *AASHTOWare* Pavement ME Design, "American Association of State Highway and Transportation Officials", Washington DC.

AASHTO (July 2008), "Mechanistic-Empirical Pavement Design Guide, A Manual of Practice", Washington DC.

AASHTO (1993) "Guide for the Design of Pavement Structures, American Association of State Highway and Transportation Officials"

Asphalt Institute (1981) "Asphalt Pavements for Highways and Streets", Asphalt Institute Manual Series-1 (MS-1), 9th Edition.

Dempsey, B.J., W.A. Herlach and J. Patel, (1985) "The Climatic Material-Structural-Pavement Analysis Program, Federal Highway Administration", Final Report Vol. 3., FHWA-RD-84-115.

FHWA (2001). ''Traffic Monitoring Guide'' U.S. Department of Transportation, Federal Highway Administration, Office of Highway Policy Information, Washington, DC.

Khazanovich, L. H.T. Yu, S. Rao, K. Galasova, E. Shats and R. Jones, (2000). "ISLAB 2000-Finite Element Analysis Program for Rigid and Composite Pavements"; User's Guide, ERES Division of ARA Inc., Champaign, IL.

Kim, S. H. Ceylan, D. Ma, and K. Gopalakrishnan, (2013) "Local Calibration Studies on DARWin-ME/Mechanistic-Empirical Pavement Design Guide Jointed Plain Concrete Pavement Performance Prediction Models", Transportation Research Board, Paper 13-2667.

Liu, H.S. and R.L. Lytton, (1985) "Environmental Effects on Pavement Drainage", Volume IV, Federal Highway Administration, Report FHWA-DTFH-61-87-C-00057.

Long Term Pavement Performance, Federal Highway Admin, www.tfhrc.gov/pavement/ltpp/datapave.htm

Lytton, R.L., D.E.Pufhal, C.H.Michalak, H.S.Liang and B.J. Dempsey, (1993) "An Integrated Model of the Climatic Effect on Pavements", FHWA-RD-90-033, November.

Minnesota Road Research Project (MnRoad) www.mrr.dot.state.mn.us/research/MnROAD_Project/MnROADProject.asp

NCHRP (July 2004). ''2002 Design Guide: Design of New and Rehabilitated Pavement Structures'', Draft Final Report, National Cooperative Highway Research Program NCHRP Study 1-37A, Washington, DC.

Papagiannakis, A.T. and E.A. Masad, "Pavement Design and Materials", Wiley and Sons, Hoboken, NJ. ISBN: 978-0471214618.

Papagiannakis, A.T., M.Bracher, J.Li and N.Jackson (2006), "Sensitivity of the NCHRP 1-37A Pavement Design to Traffic Input", Journal of the Transportation Research Board Record No. 1945, pp. 49-55.

Paris, P. and F. Erdogan, (1963) "A Critical Analysis of Crack Propagation Laws, Journal of Basic Engineering", Transactions of the American Society of Mechanical Engineers, December 1963, pp.528-534.

Schwartz C.W., R. Li. H. Ceylan and S. Kim, (2013) "Global Sensitivity Analysis of Mechanistic-Empirical Performance Predictions for Flexible Pavements", Transportation Research Board, Paper 13-1572.

Tseng, K. and R.Lytton, (1989) "Prediction of Permanent Deformation in Flexible Pavement Materials. Implications of Aggregates in the Design, Construction and Performance of Asphalt Pavements", ASTM STP 1016, pp. 154-172, American Society for Testing of Materials.

Uzan, J., (2001) "Jacob Uzan Layer Elastic Analysis" (JULEA) Software.

Von Quintus, H.L., (1994) "Performance Prediction Models in the Superpave Mix Design System", Strategic Highway Research Program, Report SHRP-A-699, WesTrack; Accelerated Field Test of Performance-Related Specifications for Hot-Mix Asphalt Construction, FHWA Contract No. DTFH61-94-C-00004, www.westrack.com/

Witczak, M.W., R.Roque, D.R.Hiltunen, W.G.Buttlar, (2000) "Modification and Re-calibration of Superpave Thermal Cracking Model", Superpave Support and Performance Models Management, Project Report NCHRP Project 9-19, Project Deliverable Task B.